# Mt. Kelud haze removal using color attenuation prior

# Mt. Kelud haze removal using color attenuation prior

**Fresy N[1,2,a], Eko M Yuniarno[1,b], Supeno M S N[1,c] and M Hariadi[1,d]**

[1]Electrical Engineering Department, Faculty of Industrial Technology, Sepuluh Nopember Institute of Technology (ITS), Surabaya, Indonesia
[2]Information Technology Department, Faculty of Science and Technology, Islamic State University (UIN) Maulana Malik Ibrahim, Malang, Indonesia

Email: [a]fresy14@mhs.ee.its.ac.id, [b]ekomulyanto@ee.its.ac.id, [c]mardi@ee.its.ac.id, [d]mochar@ee.its.ac.id

**Abstract**. Kelud crater observation using closed-circuit television (CCTV) has not been used as the main guide in the world of volcanology. This is caused by observations manually by volcanologist who is not certain and depends on their ability and experience. In practice, there is still obstacles haze in the image taken from CCTV record. This paper present color attenuation prior method to eliminate haze on the digital image. The results obtained showed that the selected method is capable of eliminating sparse haze and moderate haze but not dense haze.

## 1. Introduction

Concerning about the Mt. Kelud eruption has become central issues in preparedness and mitigation, as a result, much research in recent years has focused on the development of early warning system to observe pre-eruption activity. One of the most important parameters to be observed is the crater lake. Researchers have studied and improved many aspects of the crater lake monitoring at Mt. Kelud. Hidayati et al.[1] responded to the need for detection before the eruption based on color changes to determine the distribution of the crater lake hiposentrum, and Bernard [2] based on water sampling directly of the crater lake, Nandaka and Agung [3] has added a device such as CCTV to observe the smoke activity before eruption. These phenomena known as high activity in the crater lake. It occurs when a perfect mixture of gases ($SO_2$, HCl, HF and $CO_2$) from the bottom of the crater lake is strong enough to penetrate the depths of the lake, until it pops out of the lake in the form of a puff of smoke [4]. In this case, the observations of the smoke can be performed using pattern recognition of images taken from the permanent CCTV which is mounted on the side of the volcano's crater lake. Pattern recognition is an objective statistical approach that used for geophysical problems [5,6] search for general patterns in precursory activity before the eruption (e.g., smoke)[7]. However, the resulting CCTV images are visually ineffective due to the haze along the day and it's different thickness. Therefore, this paper proposes a method to remove haze in a single image taken from CCTV, before detecting smoke in the digital image.

During the last twenty years, haze removal techniques were successfully elaborated [8-27]. Initial attempts focused on contrast enhancement of a single image using histogram equalization [8-10]. These methods are time-consuming and are often technically difficult to perform. Some improved algorithms[11-13] suggested a possible instant haze removal of multiple images based on polarization. Unfortunately, these methods do not consider different weather conditions. Therefore, Narasimhan et

al. improved haze removal approaches for different weather [14-16]. Tan [17] refined visibility in bad weather from a single image based on Markov Random Field.

In terms of haze removal of color images, [18] proposes independent component analysis (ICA), however, it is difficult to deal with dense-haze images. He et al. [19] suggest the dark channel prior (DCP) approach for non-sky images based one color channel. There remains a need for an efficient method that can handle sky images for color images. Zhu et al. [20-21] propose color attenuation prior for single image haze removal based on a supervised learning method to create a linear model for the scene depth of the hazy image. With the recovered depth information, it can easily remove the haze from a single hazy image.

The purpose of this study is to examine the color attenuation prior to remove haze in a hazy single image which is taken using CCTV. The main body of this paper is divided into three sections. Section 2 consists of a short literature survey. Section 3 begins to apply of the color attenuation prior method at the crater lake single image. Section 4 describes and discusses the result.

## 2. Haze Removal

Haze removal is a challenging area of research. Among others, Tan [22] observation stated that the haze-free image more contrast than the image containing haze, and be able to maximize the contrast in a local region of the input image. Fattal [23] were able to achieve good results by assuming that the transmission and shadows on the surface locally unrelated. Finally, a very good approximation filed He et al., in which they use dark pixels in the local window dark pixels to produce a rough estimate of the transmission map [24] that obtain results exceeding other algorithms and even managed to dense haze. Several refinement algorithms [25–31], [40–46] are suggested to cope with the shortcoming of the DCP approach. For more efficiency, Gibson et al. [26], Yu et al. [27], He et al. [38], Tarel and Hautiere [40], and Tarel et al. [41] substitute the slow process of soft matting [39] with median filtering, “median of median filter”, guided joint bilateral filtering [32–37] and guided image filtering, successively.

### *2.1. Haze Model*

The visual field of computers and computer graphics, mathematical models used to describe the formation of haze is: [14,15,18,21]

$$\boldsymbol{I}_{(x)} = \boldsymbol{J}_{(x)} t_{(x)} + \boldsymbol{A}(1 - t_{(x)}) \tag{1}$$

Where $\boldsymbol{I}_{(x)}$ is the image observed, $\boldsymbol{J}_{(x)}$ is part of the lighting (haze), $\boldsymbol{A}_{(x)}$ is the light of the global atmosphere and $t_{(x)}$ is the portion of light that reaches the camera. $(x) = (x, y)$ is a 2D vector correspond to the coordinates (x, y) of a pixel position in the image. The purpose of detection is to eliminate noise $t_{(x)}$ where $0 < \boldsymbol{I}, \boldsymbol{J}, \boldsymbol{A}, t_{(x)} < \infty$. As shown in Figure 1.

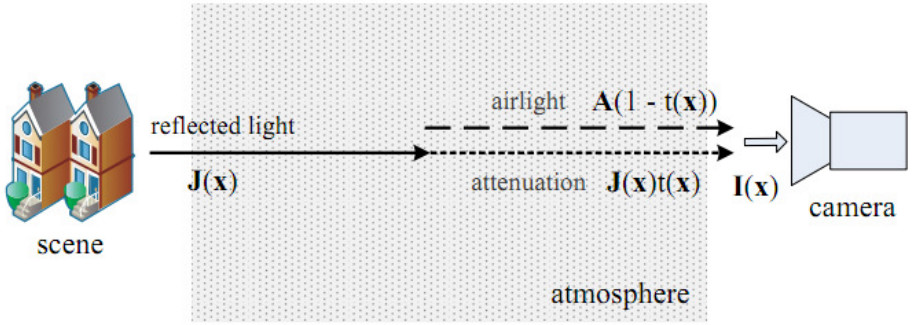


**Figure 1.** A macro physical picture of the haze imaging model.[14]

In the mathematical model $\boldsymbol{J}_{(x)}\ t_{(x)}$ is called direct attenuation, whereas $\boldsymbol{A}\ (1\text{-}t_{(x)})$ describes the airlight [15]. Attenuation directly describes the lighting section which causes damage to the image, while the airlight generated from the scattered light and causing the image of the color shift. At the moment the atmosphere is homogeneous, then the transmission of $t_{(x)}$ can be modeled by: [21]

$$t_{(x)} = e^{-\beta d(x)} \tag{2}$$

Where $\beta$ is a coefficient indicating the spread of the atmosphere on the lighting value exponentially with the depth of the image *(d)*. Geometrically, in equation (2), may imply that in the RGB-type image, vector $\boldsymbol{A}_{(x)}$, $\boldsymbol{I}_{(x)}$ and $\boldsymbol{J}_{(x)}$ is coplanar and end point parameters are collinear. Transmission $t_{(x)}$ is the ratio of the two line segments:

$$t_{(x)} = \frac{\|\boldsymbol{A}_{(x)} - \boldsymbol{I}_{(x)}\|}{\|\boldsymbol{A}_{(x)} - \boldsymbol{I}_{(x)}\|} \tag{3}$$

2.2. *Color Attenuation Prior*

It can be concluded from this context that the effect of the white or gray airlight on the observed values is additive. Thus, caused by the airlight, the brightness are increased while the saturation is decreased. It allows us to take advantage of the difference between the brightness and saturation to estimate the concentration of the haze. Since the haze concentration increases along with the change of the scene depth, then the depth of the scene is positively correlated with the concentration of the haze. This relation can be regarded as color attenuation prior, and written as: [20,21]

$$d(\mathrm{x}) = \theta_0 + \theta_1 v(\mathrm{x}) + \theta_2 s(\mathrm{x}) + \varepsilon(\mathrm{x}) \tag{4}$$

where x is the position within the image, $d$ is the scene depth, $v$ is the brightness component of the hazy image, $s$ is the saturation component, $\theta_0$, $\theta_1$, $\theta_2$ are the unknown linear coefficients, $\varepsilon(\mathrm{x})$ is a random variable representing the random error of the model, and $\varepsilon$ can be regarded as a random image.

*2.3. Image Quality Assessment*

Image quality assessment conducted by an objective assessment by using the amount of *Mean Square Error* (MSE) and *Peak Signal to Noise Ratio* (PSNR), both of these quantities are used to compare the pixels at the same position of the two different images. MSE is the average squared error between the original image with the image processing result which can be formulated as follows:

$$MSE = \frac{1}{MN}\sum_{x=0}^{M-1}\sum_{y=0}^{N-1}\left|\left(f(x,y) - g(x,y)\right)^2\right| \tag{5}$$

PSNR is the value ratio between the maximum value color image on filtering results with the quantity of interference (noise), which is expressed in decibels (*dB*), noise is the average root mean squared error $(MSE)^{1/2}$. Mathematically, PSNR can be formulated as follows:

$$PSNR = {}^{10}\log 10\left(\frac{255}{(MSE)^{1/2}}\right) \tag{6}$$

## 3. Method

Tests performed on a single image of the crater of Mt. Kelud, which was taken in May 2016 belonged to the meteorology agency in East Java, with a size of 800 x 450 pixels. The single image of the crater of Mt. Kelud consist of a sparse hazy image, a moderate hazy image and a dense hazy image. Each performed at different β values, namely $\beta_1 = 1.1$, $\beta_2 = 1.2$, $\beta_3 = 1.4$, $\beta_4 = 1.6$, $\beta_5 = 1.8$ and $\beta_6 = 1.9$.

In figure 2 it can be seen that the color of single images, on the CCTV crater lake, uses the RGB model to determine color. Once the camera has read these values, they are transformed to HSV

values.The HSV model depicts colors similarly as the human eye tends to perceive color. RGB defines color in terms of a combination of primary colors, while, HSV delineates color using common comparisons such as color, vibrancy and brightness.


**Figure 2**. The left image is the hazy image before color attenuation prior method, and the right is the result of haze removal.

Hue represents the color type. Saturation represents the vibrancy of the color. The value represents the brightness of the color. For example, white has an HSV value of 0-255, 0-255, 255. Black has an HSV value of 0-255, 0-255, 0. The HSV values are then used in the code to incorporate additional information from a given guidance image during the filtering process. The filtering output is locally a linear transform of the guidance image. Hereinafter, the filtering output is refined.

## 4. Results and Discussion

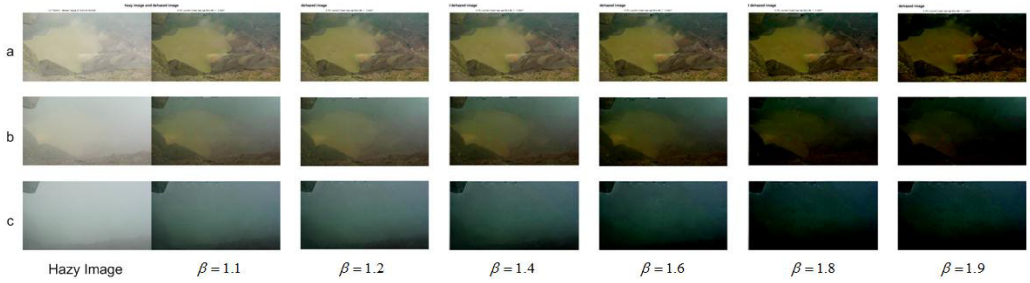


**Figure 3**. The left image is the hazy image before color attenuation prior method, and the right is the result of haze removal in the case of $\beta_1 = 1.1$, $\beta_2 = 1.2$, $\beta_3 = 1.4$, $\beta_4 = 1.6$, $\beta_5 = 1.8$ and $\beta_6 = 1.9$. (a) A sparse hazy image, (b) a moderate hazy image and (c) a dense hazy image, respectively.

From figure 3 it can be seen that the greater the value of $\beta$, the more dark haze removal results obtained. In these trials, for the sparse haze image (a), the beta value of which still look natural, $\beta_1 = 1.1$, $\beta_2 = 1.2$, $\beta_3 = 1.4$, $\beta_4 = 1.6$. For the moderate haze image (b), the value of $\beta$ for the natural results of haze removal is $\beta_1 = 1.1$, $\beta_2 = 1.2$, $\beta_3 = 1.4$,. Meanwhile, For the dense haze image (c), using the same beta value, the method can not remove the haze. Based on these trials, the proposed method, capable of eliminating the sparse haze, and the moderate haze only but not the dense haze.

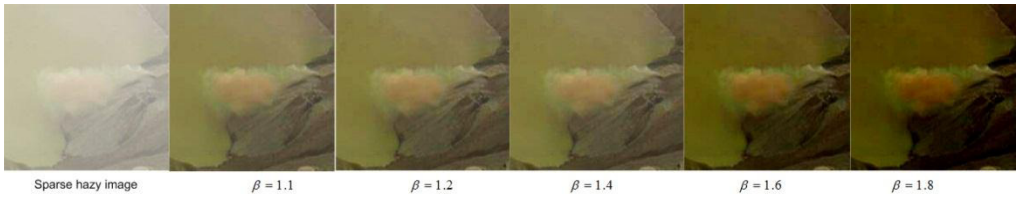


**Figure 4** A closer look at the sparse hazy image after haze removal in the case of $\beta_1 = 1.1$, $\beta_2 = 1.2$, $\beta_3 = 1.4$, $\beta_4 = 1.6$ and $\beta_5 = 1.8$. The left image is the hazy image before color attenuation prior method.

Figure 4 gives, a comparison of the result of the haze removal using different β for the sparse hazy image. The natural result is for β = 1.1, β =1.2, β = 1.4. Whereas for β =1.6 and β =1.8, the image less bright than the beta value which is previously mentioned.

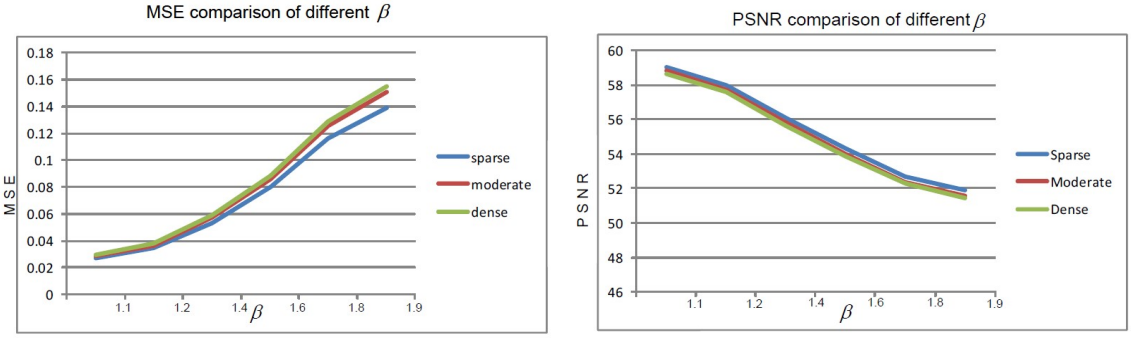


(a) (b)

**Figure 5** A comparison of (a) MSE and (b) PSNR in the case of $\beta_1$= 1.1,$\beta_2$=1.2, $\beta_3$=1.4, $\beta_4$=1.6, $\beta_5$ =1.8 and $\beta_6$ =1.9.

From figure 5, it can be seen that the higher β value, the MSE (a) is also increasing. Although the line for moderate haze and dense haze coincident but the results are different. As shown in figure 3. Meanwhile, the higher $\beta$ value, the PSNR (b) is decreasing.

## 5. Conclusion

In this study, we have applied the color attenuation prior method to remove the haze of the single image taken from Mt. Kelud crater lake. The preliminary results show that this method works properly for sparse haze and moderate haze. The drawback of this method is it can not work properly for dense haze. In the future, we will do further investigation in order to enhance the ability of this method.

## References

[1] Hidayati S, Basuki A, Kristianto and Mulyana I December 2009 *Jurnal Geologi Indonesia***4** No. 4 229-38.
[2] Bernard A 25th to 31st July 2013 IAVCEI Commission of Volcanic Lakes 8th *Workshop onVolcanic Lakes*, Aso volcano and Hokkaido Island, JAPAN.
[3] Nandaka and Agung I G M May 24th-28th 2015 *Japan Geoscience Union Meeting*, Makuhari, Chiba, Japan.
[4] Pasternack G B and Varekamp J C 1997 *Bull. Volcanol* **58** 528–38.
[5] Sandri L, Marzocchi W and Zaccarelli L 2004 *Bull. Volcanol* **66** 263–75.
[6] Sandri L, Marzocchi W and Gasperini P 2005 *Geophys. J. Int.***163** 1203–18.
[7] Rosas A T M and Reyna S D C 2008 *J. Volcanol. Geotherm. Res.* **176** 277–90.
[8] Kim T K, Paik J K, and Kang B S Feb 1998 *IEEE Trans. Consum. Electron*. **44** no. 1 pp. 82– 7.
[9] Stark J A May 2000 *IEEE Trans. Image Process.* **9** no. 5 pp. 889–96.
[10] Kim J Y, Kim L S and Hwang S H Apr 2001 *IEEE Trans. Circuits Syst. Video Technol.* **11** no. 4 pp. 475–484.
[11] Schechner Y Y, Narasimhan S G and Nayar S K 2001 *Proc. IEEE Conf. Comput. Vis. PatternRecognit. (CVPR)* pp. I-325–I-332.
[12] Shwartz S, Namer E and Schechner Y Y 2006 *Proc. IEEE Conf. Comput. Vis. Pattern*

*Recognit.(CVPR)* **2** pp. 1984–91.
[13] Schechner Y Y, Narasimhan S G and Nayar S K 2003 *Appl. Opt.* **42** no. 3 pp. 511–525.
[14] Narasimhan S G and Nayar S K Jun 2000 *Proc. IEEE Conf. Comput. Vis. Pattern Recognit.(CVPR)* pp. 598–605.
[15] Nayar S K and Narasimhan S G Sep 1999 *Proc. IEEE Int. Conf. Comput. Vis. (ICCV)* **2** pp. 820-27.
[16] Narasimhan S G and Nayar S K Jun 2003 *IEEE Trans. Pattern Anal. Mach. Intell.* **25** no. 6 713–24.
[17] Tan R T Jun 2008 *Proc. IEEE Conf. Comput. Vis. Pattern Recognit. (CVPR)* pp. 1–8.
[18] Fattal R Aug 2008 *ACM Trans. Graph.* **27** no. 3 p. 72.
[19] He K, Sun J and Tang X Dec 2011 *IEEE Trans. Pattern Anal. Mach. Intell.* **33** no. 12, pp. 2341–53.
[20] Zhu Q, Mai J and Shao L 2014 *Proc. Brit. Mach. Vis. Conf. (BMVC)* (Nottingham, U.K) pp. 1–10.
[21] Zhu Q, Mai J and Shao L November 2015 *IEEE Trans. Image Process.* **24** No. 11 pp. 3522-33.
[22] Tan R 2008 *Proc. IEEE Conference* on *Computer Vision and Pattern Recognitio CVPR 2008* Jun. pp. 1 –8.
[23] Fattal R August 2008 *ACM Transactions on Graphics* **27** no. 3.
[24] He K, Sun J and Tang X 2009 *Proc. IEEE ComputerSociety Conference on Computer Vision and Pattern Recognition* **0** pp. 1956–63.
[25] Pei S C and Lee T Y Sep/Oct 2012 *Proc. 19th IEEE Conf. Image Process. (ICIP)* pp. 957–960.
[26] Gibson K B, Vo D T and Nguyen T Q Feb 2012 *IEEE Trans. Image Process.* **12** no. 2 pp. 662–73.
[27] Yu J, Xiao C and Li D Oct 2010 *Proc. IEEE 10th Int. Conf. Signal Process. (ICSP)* pp. 1048–52.
[28] Pulung N A, Eko M Y, M Hariadi and Valentijn V May 10-12 2012 *International Conference On Multimedia Computing and System (ICMCS'12)* (Movenpick, Tangier, Morocco).
[29] Zhu Q, Yang S, Heng P A and Li X Dec. 2013 *Proc. IEEE Conf. Robot. Biomimetics (ROBIO)* 1796–00.
[30] Xiao C and Gan J Jun. 2012 *Vis. Comput.* **28** nos. 6–8 pp. 713–721.
[31] Xiang Y, Sahay R R and Kankanhalli M S Jul. 2013 *Proc. IEEE Conf. Multimedia ExpoWorkshops (ICMEW)* pp. 1–4.
[32] Tomasi C and Manduchi R Jan 1998 *Proc. 6th Int. Conf. Comput. Vis. (ICCV)* pp. 839–46.
[33] Paris S and Durand F 2006 *Proc. Eur. Conf. Comput. Vis.* pp. 568–80.
[34] Porikli F Jun 2008 *Proc. IEEE Conf. Comput. Vis. Pattern Recognit. (CVPR)* pp. 1–8.
[35] Yang Q, Tan K H and Ahuja N Jun 2009 *Proc. IEEE Conf. Comput. Vis. Pattern Recognit.(CVPR)* pp. 557–64.
[36] Adams A, Gelfand N, Dolson J, and Levoy M 2009 *Proc. ACM SIGGRAPH* pp. 21:1–21:12.
[37] Adams A, Baek J and Davis M A May 2010 *Comput. Graph. Forum* **29** no. 2 pp. 753–62.
[38] He K, Sun J and Tang X Jun 2013 *IEEE Trans. Pattern Anal. Mach. Intell.* **35** no. 6 pp. 1397–09.
[39] Levin A, Lischinski D and Weiss Y Feb 2008 *IEEE Trans. Pattern Anal. Mach. Intell.* **30** no. 2 pp. 228–42.
[40] Tarel J P and Hautiere N Sep/Oct 2009 *Proc. IEEE 12th Int. Conf. Comput. Vis. (ICCV)* pp. 2201–08.
[41] Tarel J P, Hautiθre N, Caraffa L, Cord A, Halmaoui H and Gruyer D Apr 2012 *IEEE Intell.Transp. Syst. Mag.* **4** no. 2 pp. 6–20.
[42] Ancuti C O, Ancuti C, Hermans C and Bekaert P 2010 *Proc. Asian Conf. Comput. Vis. (ACCV)* 501–14.
[43] Prapti K N, Eko M Y, Supeno M S N 12 September 2015 *Seminar Nasional Pendidikan Teknik Informatika (SENAPATI 2015)* ISSN 2087-658 (Denpasar, Bali).

[44] Nishino K, Kratz L and Lombardi S Jul 2012 *Int. J. Comput. Vis.* **98** no. 3 pp. 263–78.
[45] Meng G F, Wang Y, Duan J, Xiang S and Pan C Dec 2013 *Proc. IEEE Int. Conf. Comput. Vis.(ICCV)* pp. 617–24.
[46] Tang K, Yang J and Wang J Jun 2014 *Proc. IEEE Conf. Comput. Vis. Pattern Recognit.(CVPR)* pp. 2995–02.